Extended Abstracts of the 2020 International Conference on Solid State Devices and Materials, VIRTUAL conference, 2020, pp115-116

B-10-06 (Late News)

Designing a filament in resistive random access memory based on thermal flow control

Yuta Sasaki[1] and Kentaro Kinoshita [1]

[1] Tokyo Univ. of Sci.
6-3-1 Niijuku, Katsushika-ku, Tokyo, 125-8585, Japan
Phone: +81-3-5876-1399, E-mail: 1519517@ed.tus.ac.jp

Abstract

For putting resistive random access memory (ReRAM) into variety of attractive applications, the guideline of device structure for controlling memory characteristics is required. In this paper, by adopting a combination of Soret and Fick diffusions as driving forces of Vo's in ReRAM, we demonstrated that reciprocating motion of Vo's accompanied with resistive switching could be induced. This model is consistent with good cycling endurances of unipolar-type ReRAM ever reported. Based on the model, it was clearly shown that thermal design of device including electrodes (ELs) are crucial in tuning memory characteristics, controlling the balance of the two driving forces.

1. Introduction

It is widely received that resistive switching of ReRAM is caused by formation and rupture of conductive filament (CF) consisting of Vo in the MO film of EL/MO/EL devices. However, driving forces that migrate Vo's have not been elucidated yet. Some groups reported that unipolar-type switching can be repeated by electric field drift and Fick diffusion of Vo's [1]. In these models, set switching is caused by the electric field drift of Vo's that works one-way toward the anode, and Vo's should pile up near the anode after repeating set switching. This seems to worsen the switching endurance inconsistent with good endurance of more than 10^6 cycles [2]. Therefore, two competing driving forces of Vo's that realize reciprocating movement of Vo's should be adopted to ensure high reproducibility of CF.

In this paper, we examined Soret diffusion which works in the direction of the temperature, *T*, gradient. Vo migration simulation using Soret diffusion and Fick diffusion which works in the direction of the gradient of Vo concentration.

2. Experiment

Simulation on Vo migration was performed using finite element method (COMSOL Multiphysics Ver.5.4). We used a cylindrical EL/MO/EL device with the *z*-axis as symmetric axis (Fig.1). The value of *n* was defined as the ratio of Vo concentration (n_{Vo}) to that in the MO film outside the filament region in the initial state (n_0), where n_0 is 5.43×10^{18} cm^{-3}. CF consisting of Vo's with the radius of 5 nm was located along the *z*-axis in the MO layer. As an initial condition, Vo's that consist CF obey Gaussian distribution with maximum *n* of 1000 and *r* at which *n* = 800 is defined as the radius of CF, as shown in Fig.2(a).

Vo migration induced by Fick diffusion ($\propto \nabla n$) and Soret diffusion ($\propto \nabla T$) were estimated by solving continuity equation,

$$\frac{\partial n}{\partial t} = -\nabla \cdot (D_{\mathrm{V}}\nabla n - D_{\mathrm{V}}S_{\mathrm{V}}n\nabla T), \quad (1)$$

where D_{V}, S_{V}, and k_B are the diffusion, Soret, and Boltzmann constants, respectively. Additionally, the electrical conductivity was given by $\sigma = \sigma_0 \exp(E_a/k_B T)$. Here, σ_0, electric activation energy E_a, and thermal conductivity κ were assumed to depend on *n* as shown in Fig.2(b)-(d), respectively.

Pt ($\kappa = 70$ [W/mK])and W($\kappa_{\mathrm{W}} = 174$ [W/mK]) were used as ELs.

Reset and set switching were attempted respectively by injecting saw-tooth shape voltage (SSV) pulses shown in the inset of Fig. 3: SSV pulse with height and rising time of 1 V and 1 ms was injected for reset, whereas SSV pulse with height and rising time of 3 V and 1 μs was injected for set.

3. Result and Discussion

Figs. 3(a)-(c) show *n*-distributions of Pt-EL/MO/Pt-EL devices after 1st set, 1st reset, and 2st set switching, respectively. Here, resistance after each switching was 232, 1531, and 274 Ω, respectively. Figs. 3(d)-(f) show enlarged views around the edge of CF at TE side. It is shown that CF gets not only thinned in *r* direction but also shrunk in *z* direction after reset.

Figs. 4 show Vo migration during reset ($t = 0.8$ ms) and set ($t = 1$ μs) in Pt-EL/MO/Pt-EL (left) and W-EL/MO/W-EL (right) devices. Arrows are vectors that represent the direction and strength of the flux of Vo's at the location where starting point of each vector is located. It is confirmed that Vo migrate outward and inward in *r* direction during reset and set switching as shown in Figs. 4(a) and (b), respectively. It is worth noting that Vo's migrate inward in *z* direction as well. The tendency is more prominent in the W/MO/W device than in the Pt/MO/Pt device.

Fig.5 shows *n* distribution along *z*-axis in the MO layer after reset transition. Apparently, CF becomes thin near the EL/MO interface than the other region. This result allows us to interpret that reset transition occurs in the MO layer dominantly near the EL interfaces as a result of Vo migration in the direction vertical to ELs from the vicinity of EL toward the center of the device (*z* = 30 nm).

These results indicate that large thermal conductivity of EL causes the heat flow from MO to EL especially near the EL interface. As a result, d*T*/d*z* becomes large, enhancing the Soret diffusion in the direction vertical to the EL. If we use ELs with large κ, Vo migration in *z* direction becomes prominent. These results are never obtained from one dimensional calculation considering the radial direction of the cylindrical cell only [3][4].

4. Conclusions

Repeatable resistive switching was successfully reconstructed by the simulation adopting Soret and Fick diffusions as driving forces of Vo migration. It was shown that Soret and Fick diffusion are always competing each other and large dT/dz due to the heat flow from the MO layer to Els even migrate Vo's in z direction. The present work clearly showed that thermal design of ReRAM device is crucial in tuning memory characteristics, controlling the balance of Soret and Fick diffusions.

References

[1] S. Yu, et al, IEEE EDL, 31, 1455 (2010).
[2] I.G. Beak, et al., IEDM Tech. Dig., 587 (2004).
[3] D.B. Strukov, et al., Appl. Phys. A. 102, 851 (2011).
[4] D.B. Strukov, et al., Appl. Phys. A. 107, 509 (2012).

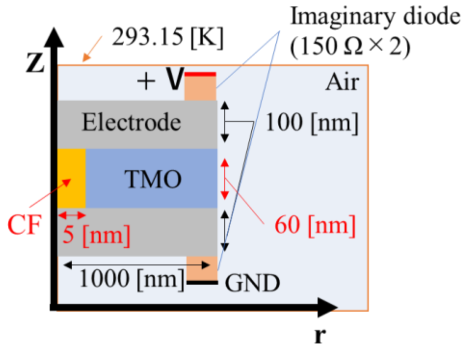

Fig. 1 Cylindrical cell used for the simulation of Vo migration.

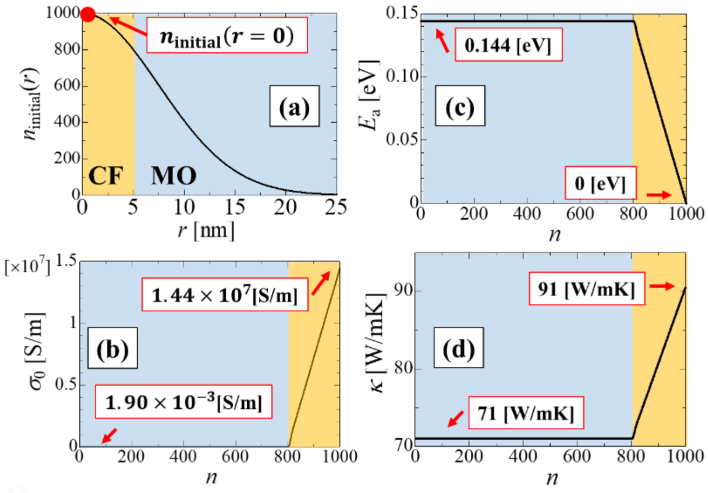

Fig. 2 Physical parameters used for metal oxide (MO) layer: (a) Initial n as a function of r. (b) electric conductivity σ_0, (c) electron activation energy E_a, and (d) thermal conductivity κ as a function of n.

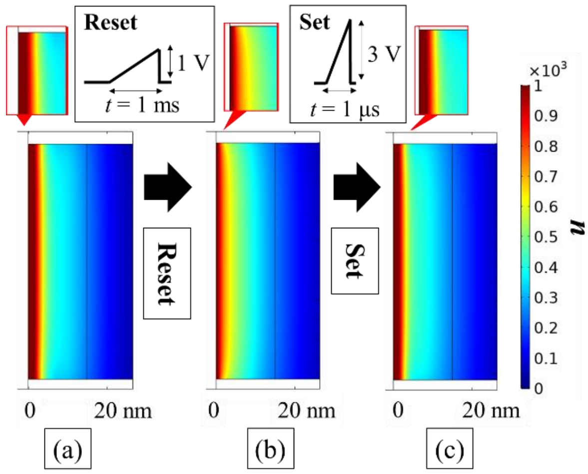

Fig. 3 n distribution in the MO layer of Pt/MO/Pt device after. (a) 1st set, (b) 1st reset, and (c) 2nd set transition.

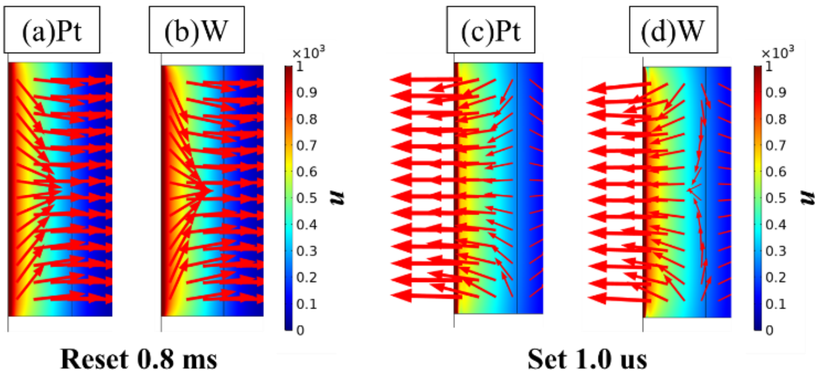

Fig.4 n distributions in the MO layer of (a) Pt/MO/Pt and (b) W/MO/W devices during reset transition (t = 0.8 ms), and those of (c) Pt/MO/Pt and (d) W/MO/W devices during set transition (t = 1.0 us). Arrows represent vectors that represent the direction and strength of the flux of Vo's.

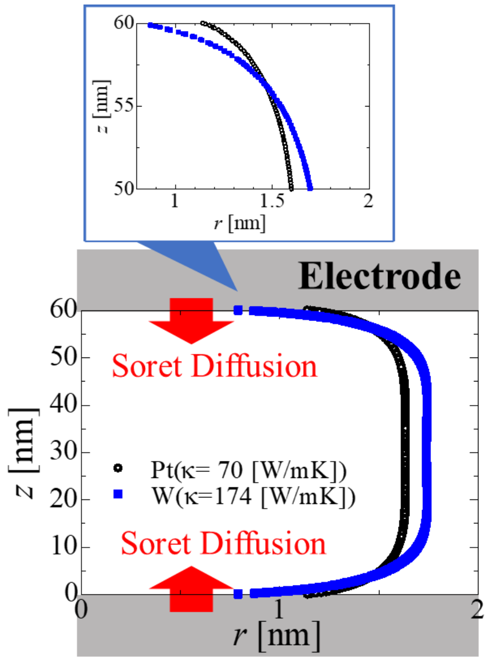

Fig. 5 n distribution along z-axis in Pt/MO/Pt (circles) and (b) W/MO/W (squares) devices after reset transition. Inset: n distribution along z-axis near the top electrode.